

Examining the Soil Responses during the Initiation of a Flow Landslide by Coupled Numerical Simulations

*Yiqiang WANG¹⁾ and Yu-Hsing WANG²⁾

^{1), 2)} *Department of Civil and Environmental Engineering, The Hong Kong University of
Science and Technology, Hong Kong, P.R. China*

¹⁾ *yqwang@ust.hk* ²⁾ *ceyhwan@ust.hk*

ABSTRACT

This paper reports the local soil responses during the initiation of flow landslide, which aims to gain insights into the associated underlying mechanisms. The FEM simulations, based on a published large-scale laboratory landslide, were carried out using a coupled framework in Abaqus for this purpose. The simulation results demonstrate that a distinct transition in the pore-water pressure development is accompanied by a sudden rise of the shear strain intensity. This can be attributed to that undrained shearing induces a sudden volumetric contraction tendency and then rises up the pore water pressure. Such an increase of the pore water pressure in turn decreases p' for those elements inside the shear band although q continues to decrease throughout the failure process. As a result, the stress paths on the $p'-q$ space of those elements inside the shear zone are towards to the critical state line whereas the stress paths of those elements outside the shear zone move away from the critical state line. All of these local responses lead to the following failure process. The shear zone starts from the bottom of the slope and then propagates towards to the top of the slopes. Ultimately, the shear zone penetrates through the whole slope for a sudden follow landslide within ~1 seconds.

1. INTRODUCTION

Rainfall-induced landslide hazards are a serious and continual problem to many places throughout the world. Among different types of landslides, flow landslides often cause heavy loss of human lives and major property damage (Anderson and Sitar 1995; Iverson 1997; Sun 1999; Hungr et al. 2001; Okura et al. 2002). In the published results, different aspects of flow landslides had been investigated (e.g., see Eckersley 1990, Rahimi et al. 2011, Chen et al. 2004). However, several critical issues related to the mechanisms that govern how sliding of slopes is triggered and then transformed into a liquefied viscous flow still remain unclear or even unknown. In addition, the local soil responses such as the associated stress path during the initiation of flow landslides are still hypothesized.

¹⁾ Postgraduate Student

²⁾ Associate Professor

It is believed that the excess pore pressures are the main factor to trigger a flow landslide. To be more explicit, the excess pores water pressure is built up after, not prior to, the initiation of failure, i.e., arising from undrained shearing. These sudden-rise excess pore pressures ultimately cause the slope soil to be liquefied and become rapid fluidized landslides (Eckersley 1990; Wang 1994; Iverson et al. 2000; Wang and Sassa 2001 and 2003; Okura et al. 2002). Such a pore-water pressure response was clearly documented in Iverson et al. (2000) where a large-scale experimental landslide was carried out. However, other local soil responses such as the stress changes were not measured in their study. Hence, the main objective of this study is to carry out a coupled numerical simulation to model the experimental in Iverson et al. (2000) and then gain insights into the associated underlying mechanisms of a flow landslide based on the additional local soil responses such as the strain and stress responses.

2. NUMERICAL PROCEDURES

In this study, the numerical simulations by the finite element method (FEM) were carried out using Abaqus (2008). The finite element meshes, the coupled formation, the adopted soil model, and the initial conditions are discussed in the following sections.

2.1. Finite element meshes and boundary conditions

Fig.1 presents the schematic diagram of the experimental setup in Iverson et al. (2000). The numerical slope follows the same geometry size in their experiment as shown in Fig. 2. A 6-node modified quadratic plane strain triangle with pore pressure and hourglass control (CPE6MP; Abaqus 2008) was used in this finite element meshes. The boundaries, AB and AD, were assumed to be undrained, and the remaining two boundaries were assumed to be drained and free of traction.

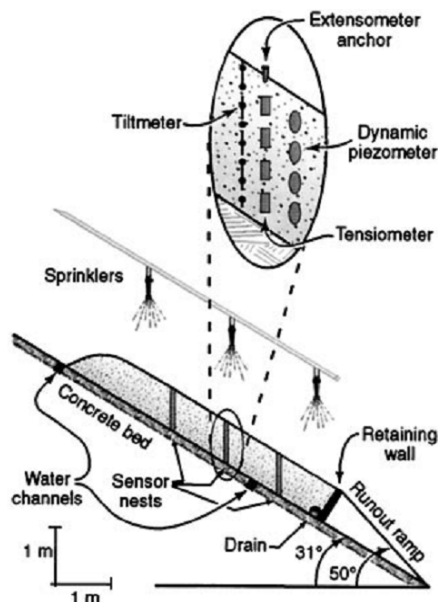


Fig. 1 Schematic diagram of the arrangement of the experimental landslide (from Iverson et al. 2000).

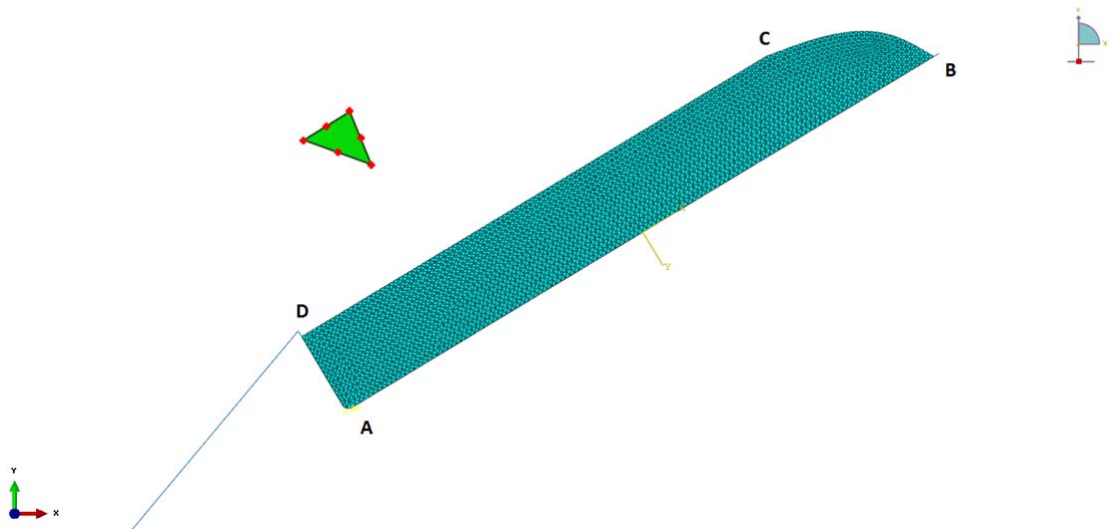


Fig. 2 Slope used in the numerical simulations and the finite element meshes.

2.2. Coupled formulation

A basic fully coupled effective-stress procedure (e.g., Biot 1941 and 1955; Zienkiewicz 1982; Zienkiewicz and Shiomi 1984) is formulated based on the physical laws of balance of linear momentum and conservation of mass as follows (the compression is assumed positive herein):

$$\sigma_{ij,j} + \rho b_i = \rho \ddot{u}_i \quad (1)$$

$$n(v_{i,i} + \dot{\varepsilon}_{vwc}) + \dot{u}_{i,i} = 0 \quad (2)$$

In Eq. (1), σ_{ij} is the total stress; ρ is bulk mass density of the soil; b_i is body force per mass; and u_i is the displacement of the soil skeleton. In Eq. (2), v is seepage velocity; ε_{vwc} is volumetric strain of the pore fluid due to compression; and n is the porosity. Eqs. (1) and (2) are coupled in that they both depend on the state variables of the soil skeleton and the pore fluid.

The constitutive law for the soil skeleton, is the modified Drucker-Prager/Cap plasticity model and the constitutive law for the seepage flow is Darcy's law with the permeability of 0.025 cm/s. In addition, the pore water pressure for unsaturated soil is quantified by the equation proposed by Bishop and Blight (1963):

$$u = u_a + \chi(u_w - u_a) \quad (3)$$

where u_w is the pore-water pressure; u_a is the pore-air pressure; χ is a parameter representing the fraction of a unit cross-sectional area of the soil occupied by water.

2.3. Modified Drucker-Prager plasticity model

The modified Drucker-Prager/Cap plasticity model (see Abaqus 2008) was used for soil model herein. The yield surface of this model includes two main segments: (1) a shear failure surface providing dominantly shearing flow and (2) a "cap," which intersects the hydrostatic stress axis (see Fig. 3 for details). There is a transition surface to bridge these two segments. The cap serves two main purposes. First, it bounds the yield surface in hydrostatic compression, thus providing an inelastic hardening mechanism for plastic compaction. Second, as the material yields due to

shearing, it helps to control volume dilatancy by providing softening response as a function of the inelastic volume increase created as the material yields on the Drucker-Prager shear failure and the transition surface. The selected parameters for the soil model, as listed in Table 1, are aimed to capture loose soil behavior.

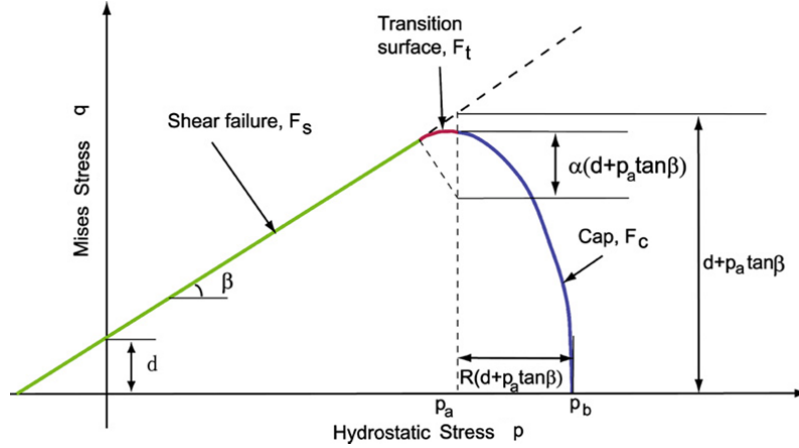


Fig. 3 Modified Drucker-Prager/Cap model: yield surfaces in the p - q plane (after Abaqus 2008).

Table 1. Parameters used in the modified Drucker-Prager/Cap plasticity model.

Elastic properties	
Young's modulus	$E = 328 \text{ MPa}$
Poisson's ratio	$\nu = 0.17$
Inelastic properties	
Material angle of friction	$\beta = 31^\circ$
Dilation angle	$\psi = 0^\circ$
Ratio of the flow stress in triaxial tension to the flow stress in triaxial compression	$K = 1.0$
Hardening behavior	
Yield stress	Absolute value of the corresponding plastic strain
0.075 MPa	0.0
0.083 MPa	0.058
0.075 MPa	0.116

2.4. Establishing the initial stress fields and the initial pore water pressure distribution

The initial stress field is given based on the elastic stress solution, and the initial pore water pressure distribution is calculated based on an assumption of the ground water table is located near the surface of the bottom concrete bed in Fig. 1, i.e., the boundary AB in Fig. 2.

3. SIMULATION RESULTS AND DISCUSSIONS

Simulation results are presented and discussed first followed by a comparison with the experimental findings in Iverson et al. (2000).

3.1. Simulation results

Fig. 4 presents failure mode of the simulated landslide at the final stage, i.e., at time $t = 2782.08$ sec. The finite element mesh is also imposed in the figure to show the initial profile of the slope as a reference. A deep shear or failure zone is observed from the FEM simulations during the development of the landslide. Fig. 5 captures the distribution of associated equivalent plastic stains in this simulated landslide at different elapsed time. The contour shows the evolution of associated equivalent plastic strains, $\frac{1}{2}(\varepsilon_1 - \varepsilon_3)$, where ε_1 and ε_3 are the principal strains (i.e., two dimensional strain invariant or called shear strain intensity in the following discussion). It can be readily seen from Fig. 5 that the shear zone starts from the bottom of the slope and then propagates towards to the top of the slopes. Finally, this shear zone suddenly goes through the whole slope within ~ 1 seconds for an acute flow landslide as found in the experiment.

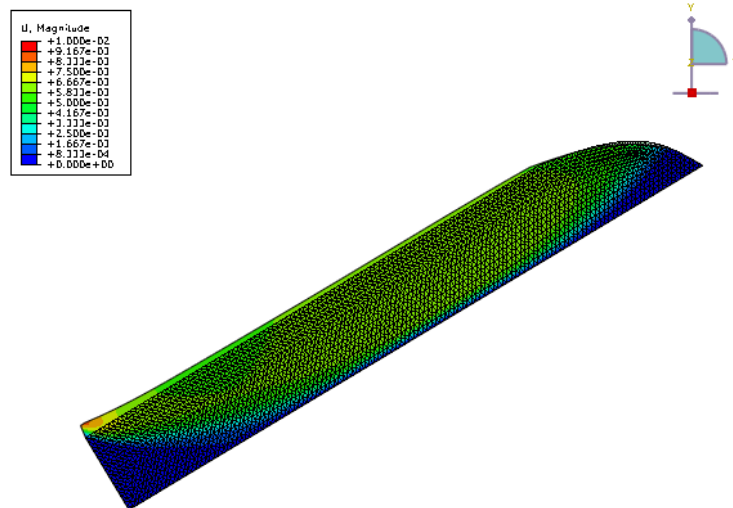
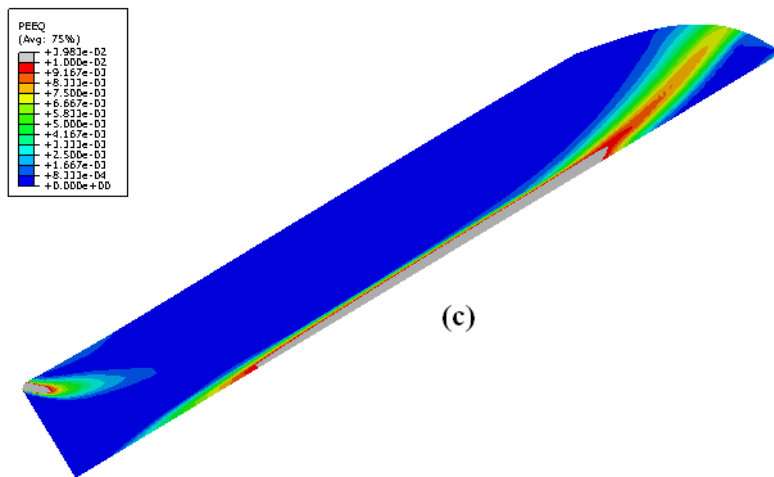
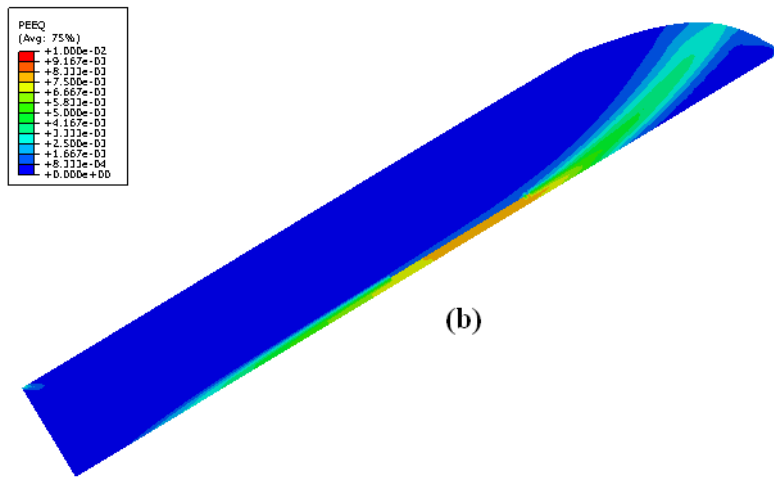
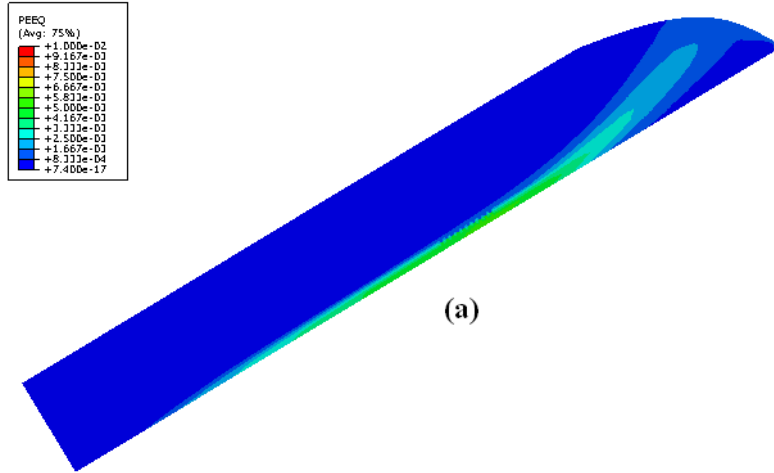


Fig. 4 Globalized failure mode obtained from the numerical simulations (Distributions of the displacement magnitude at $t = 2782.08$ sec.).



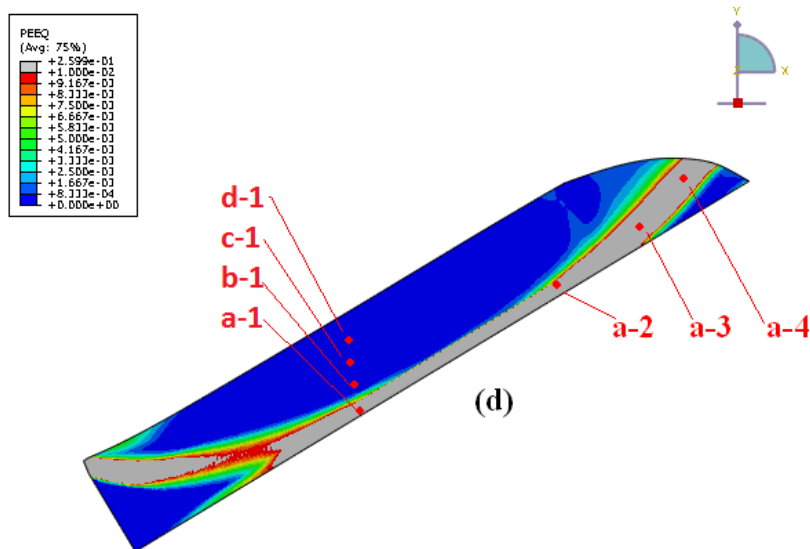


Fig. 5 Results of numerical simulations:

(a) at $t = 2601$ sec; (b) at $t = 2762$ sec; (c) at $t = 2780$ sec; and (d) at $t = 2782.08$ sec.

There are 7 nodes, as indicated in Fig. 5d, selected to examine the responses of pore water pressure at different locations. Nodes a-1, a-2, a-3, and a-4 are along the shear zone and nodes b-1, c-1, and d-1 are aligned right above nodes a-1, i.e., along the vertical soil profile. Fig. 6 presents the pore water pressure responses in those nodes along the vertical soil profile. It can be found that the corresponding pore water pressure increases more rapidly in the deep area than in the shallow area before $t < \sim 2780$ sec. After $t > \sim 2780$ sec, there is a distinct transition after which the pore water pressure at node a-1 suddenly increases. This suggests that the shear-induced pore water pressure begins to prevail, i.e., positive excess pore water pressure induced by a sudden shearing contraction in the loose slope under an undrained condition. The results in Fig. 7 can lend a further support to this suggestion based on the evolution of the equivalent plastic strain (i.e., the shear strain intensity) at node a-1, i.e., a sudden increase of the shear strain at $t \approx 2780$ sec. On the contrary, this behavior is not found in the response of nodes b-1, c-1 and d-1 because these three positions are not involved in the shear zone.

As also shown in the numerical simulations, the shear zone gradually develops towards the upper part of the slope. This observation explains the evolution of the pore water pressure and shear strain intensity in those nodes along the shear zone as shown in Figs. 8 and 9. When there is a distinct transition in the pore-water pressure development, a sudden increase of the shear strain intensity can also be found. For instance, this transition point can be identified at $t \approx 2762$ sec as indicated by a dotted line in the figure.

Figs. 10 and 11 present the associated evolution of stress paths on the p' - q space for those nodes along the vertical profile and involved in the shear zone. It can be found that the deviatoric stress q continues to decrease at most of the locations in the slope while the mean effective stress p' decreases inside the shear zone but increases outside the shear zone. This suggests that inside the shear zone the tendency of volumetric contraction (see the evidence in Figs. 7 and 9 about the changes in the

shear strain intensity) gives rise to a positive excess pore water pressure, i.e., under an undrained shearing, and therefore p' decreases. As a result, the stress paths on the $p'-q$ space for those elements inside the shear zone move towards to the critical state line during the process of slope failure whereas the stress paths for those elements outside the shear zone are away from the critical state line. In any case, the stress path is not under a constant q as suggested in Brand (1981). In addition, the decreasing p' is not mainly arising from the saturation process.

In short, once again, undrained shearing induces a sudden volumetric contraction tendency and then rises up the pore water pressure. This action in turn weakens the soil inside the shear zone by decreasing p' (although q continues to increase) and therefore the associated stress path is towards to the critical state line. The shear zone is initiated locally and then propagates to the top of the slope. Ultimately, the shear zone penetrates through the whole slope for a sudden massive failure. A flow landslide is expected to occur in an acute way owing to high pore water pressures promoting soil liquefaction.

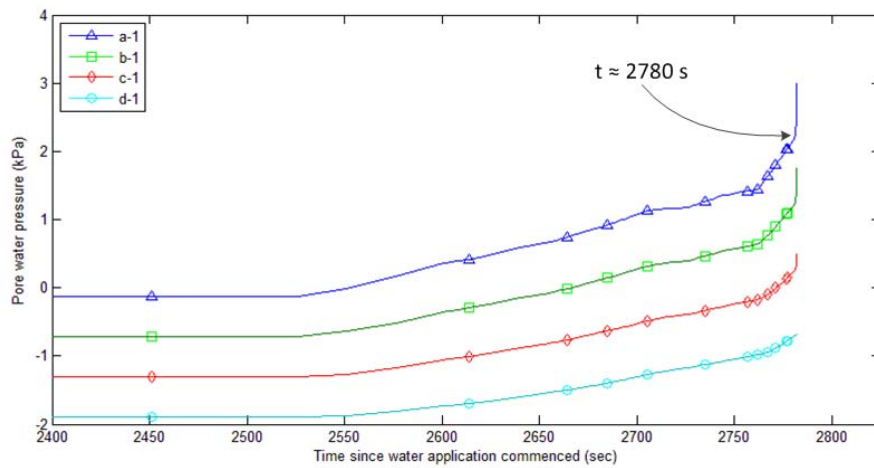


Fig. 6 Simulation results on pore water pressure commenced responses along the vertical profile of the slope.

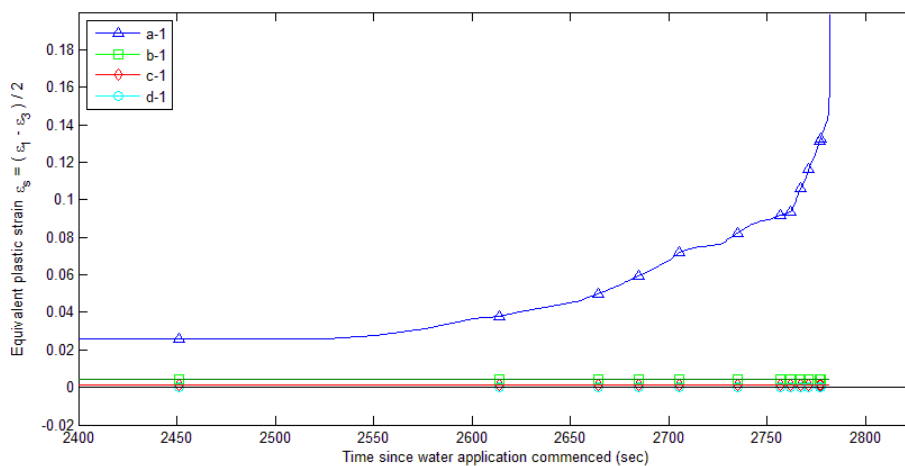


Fig. 7 Simulation results on the equivalent plastic strain responses along the vertical profile of the slope.

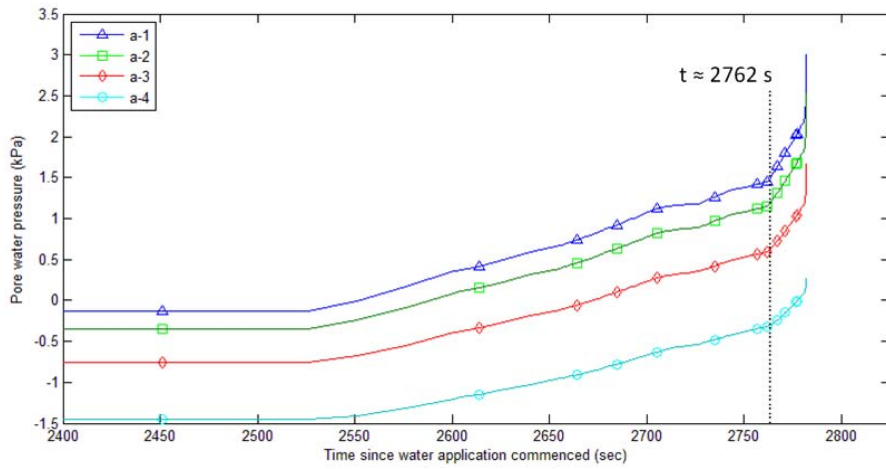


Fig. 8 Simulation results on pore water pressure responses along the shear zone.

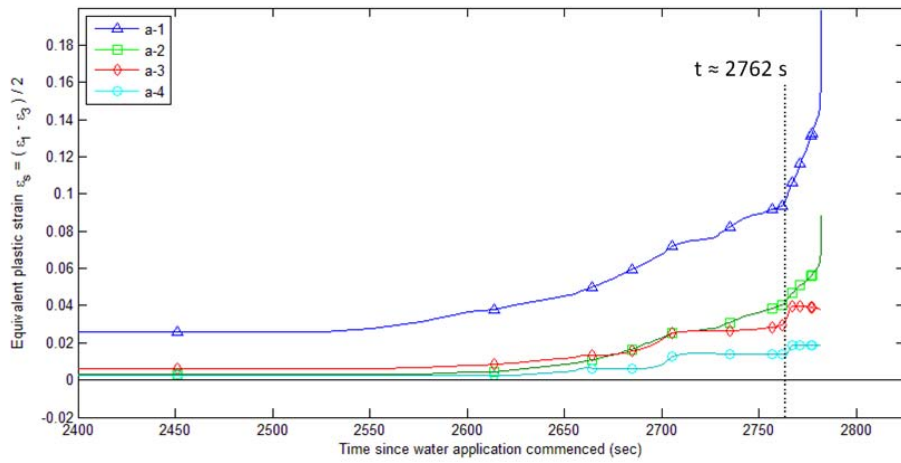


Fig. 9 Simulation results on the equivalent plastic strain responses along the shear zone.

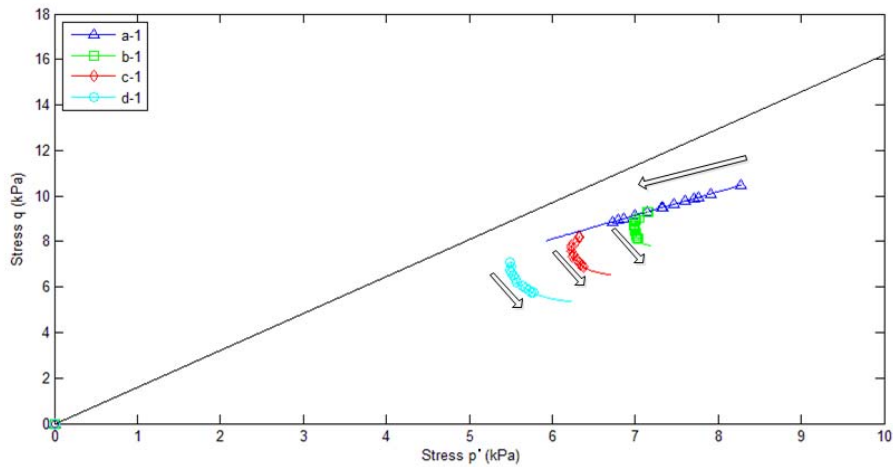


Fig. 10 Simulation results on the stress path responses along the vertical profile of the slope

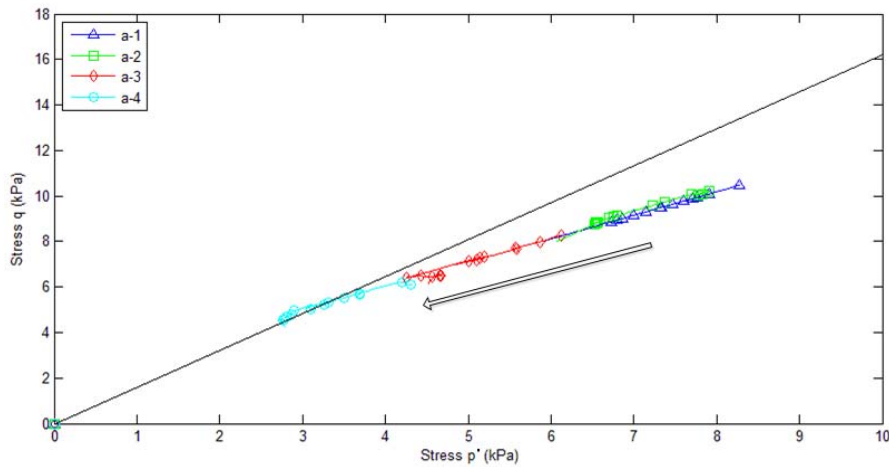


Fig. 11 Simulation results on the stress path responses along the shear zone.

3.2 Comparing with the experimental results

Fig. 12 presents the experimental results on a flow landslide taking place in a loose slope (from Iverson et al. 2000). As illustrated by Iverson et al. (2000) and Logan (2007), the failure mode is sudden and global wise. Therefore, a deep failure zone close to the bottom concrete bed is expected, which is in agreement with the numerical simulations. Also considering the quantities of pore water pressure responses, the numerical simulations with a detailed investigation and subtle adjustment can accurately capture the sudden increase of the pore water pressure induced by soil contraction as observed in the experiment.

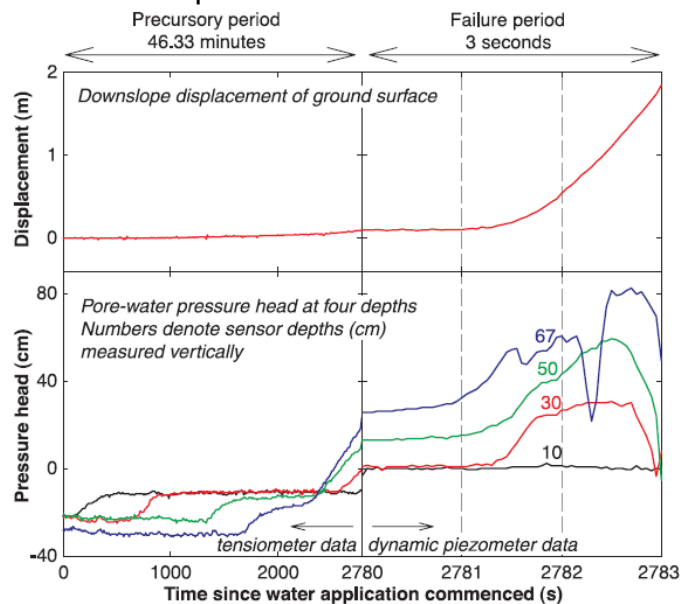


Fig. 12 Experimental results: (a) downslope displacement of ground surface and (b) pore-water pressure head at different depths (from Iverson et al. 2000).

4. CONCLUSION

The simulation results demonstrate that the shear zone starts from the bottom of the slope and then propagates towards to the top of the slopes. Finally, this shear zone suddenly goes through the whole slope within ~1 seconds for an acute flow landslide as found in the experiment done by Iverson et al. (2000). The simulation results also suggest that when there is a distinct transition in the pore-water pressure development, a sudden rise of the shear strain intensity can be found. That is, shearing induces a sudden volumetric contraction tendency under an undrained condition and then gives rise to an increase in the pore water pressure. This in turn decreases p' for those elements inside the shear zone although q continues to decrease throughout the failure process. As a result, the stress paths on the p' - q space of those elements inside the shear zone move towards to the critical state line whereas the stress paths of those elements outside the shear zone are away from the critical state line. All of these local soil responses lead to a sudden occurrence of a flow landslide. Note that the stress path is not under a constant q as generally assumed. In addition, the decreasing p' is not mainly arising from the saturation process.

ACKNOWLEDGMENTS

This research was supported by the Hong Kong Research Grants Council (GRF 621109).

REFERENCES

- Abaqus (2008). *Standard User's Manual Version 6.8-1*, Dassault Systems.
- Anderson, S.A., and Sitar, N. (1995). "Analysis of rainfall-induced debris flows." *Journal of Geotechnical Engineering*, 121(7), 544–552.
- Biot, M.A. (1941). "General theory of three dimensional consolidation." *Journal of Applied Physics*, 12, 155–164.
- Biot, M.A. (1955). "Theory of elasticity and consolidation for a porous anisotropic solid." *Journal of Applied Physics*, 26(2), 182–185.
- Bishop A.W., and Blight G.E. (1963). "Some aspects of effective stress in saturated and partly saturated soils." *Geotechnique*, 13(3), 177–197.
- Brand, E.W. (1981). "Some thoughts on rain-induced slope failures." *Proceedings of the 10th International Conference on Soil Mechanics and Foundation Engineering*, Stockholm, 3, 373–376.
- Broms, B. (1979). "Negative skin friction." *Proceedings of the 6th Asian Regional Conference on Soil Mechanics and Foundation Engineering*, Singapore, 2, 41–75.
- Chen, H., Lee, C., and Law, K. (2004). "Causative mechanisms of rainfall-induced fill slope failures." *Journal of Geotechnical and Geoenvironmental Engineering*, 130(6), 593–602.
- Eckersley, D. (1990). "Instrumented laboratory flowslides." *Géotechnique*, 40(3), 489–502.

- Hungr, O., Evans, S.G., Bovis, M.J., and Hutchinson, J.N. (2001). "A review of the classification of landslides of the flow type." *Environmental and Engineering Geoscience*, 7(3), 221-238.
- Iverson, R.M. (1997). "The physics of debris flows." *Reviews of Geophysics*, 35(3), 245-296.
- Iverson, R.M., Reid, M.E., and LaHusen, R.G. (1997). "Debris-flow mobilization from landslides." *Annual Review of Earth and Planetary Sciences*, 25, 85-138.
- Iverson, R.M., Reid, M.E., Iverson, N.R., LaHusen, R.G., Logan, M., Mann, J.E., and Brien, D.L. (2000). "Acute sensitivity of landslide rates to initial soil porosity." *Science*, 290, 513-516.
- Logan, M., and Iverson, R.M. (2007). "Video documentation of experiments at the USGS debris-flow flume 1992-2006." *U.S. Geological Survey Open-File Report*, 2007-1315.
- Okura Y., Kitahara, H., Ochiai, H., Samori, T., and Kawanami, A. (2002). "Landslide fluidization process by flume experiments." *Engineering Geology*, 66, 65-78.
- Rahimi A., Rahardjo H., Leong E.C. (2011). "Effect of antecedent rainfall patterns on rainfall-induced slope failure." *Journal of Geotechnical and Geoenvironmental Engineering*, 137(5), 483-491.
- Sun, H.W. (1999). Review of fill slope failure in Hong Kong. GEO Report No. 96, Civil Engineering Department, Hong Kong.
- Wang G., and Sassa, K. (2001). "Factors affecting rainfall-induced flowslides in laboratory flume tests." *Géotechnique*, 51(7), 587-599.
- Wang G., and Sassa, K. (2003). "Pore-pressure generation and movement of rainfall-induced landslides: effects of grain size and fine-particle content." *Engineering Geology*, 69, 109-125.
- Wang, Y.H. (1994). "A Study on the Trigger Mechanisms of Debris Flow." Master's Thesis, National Taiwan University, Taiwan.
- Zienkiewicz, O.C. (1982). "Basic formulation of static and dynamic behaviors of soil and other porous media." *Applied Mathematics and Mechanics*, 3(4), 457-468.
- Zienkiewicz, O.C., and Shiomi, T. (1984). "Dynamics behavior of saturated porous media: the generalized Biot formulation and its numerical solution." *International Journal for Numerical and Analytical Methods in Geomechanics*, 8, 71-96.